Combined adaptive feedback and feedforward compensation for active vibration control using Youla–Kučera parametrization

Tudor-Bogdan Airimitoaie [a,*], Ioan Doré Landau [b]

[a] *Univ. Bordeaux, Bordeaux INP, CNRS, IMS, UMR 5218, 33405 Talence, France*
[b] *CNRS, GIPSA-lab, UMR 5216, F-38402 Saint Martin D'Hères, France*

ARTICLE INFO

ABSTRACT

The combination of adaptive feedforward with adaptive feedback disturbance compensation has been suggested since a number of years as a potential solution for improving the performance of active vibration control systems. Unfortunately, as shown in the present paper there is a strong coupling between adaptive feedback and adaptive feedforward which may lead to instabilities and new algorithms which take into account this interaction are proposed in the paper. These algorithms take advantage of the Youla-Kučera parametrization of the feedback controller and feedforward compensator. First, the adaptive feedback algorithm is presented alone. Then, the adaptive feedforward algorithm is designed taking into account the feedback controller's presence in the loop. Stability of the complete scheme is obtained by appropriately filtering the regressor vectors in order to take into account a strictly positive real condition. Experimental results obtained on a relevant test-bench illustrate the performance of this approach to active vibration control. Comparison with adaptive feedback alone, with adaptive feedforward alone and adaptive feedforward + fixed feedback are provided.

© 2018 Elsevier Ltd. All rights reserved.

1. Introduction

Two approaches have been considered for adaptive ANVC: *feedforward compensation* and *feedback compensation*. Historically, the feedforward compensation approach has been used first. This approach requires the use of an additional transducer providing information upon the disturbance and is subject to the presence of an unwanted "positive" feedback coupling between the compensator system and the measurement of the disturbance (see also [1] for ANC and [2] for AVC). Despite these difficulties, this approach is systematically used when information upon the disturbance is available and when the disturbance is broadband since from a control point of view the level of compensation is not limited by a Bode integral constraint as is the case in feedback compensation.

The use of the feedback compensation is more recent. It uses the internal model principle (IMP) and it is particularly suitable for narrow-band disturbances [2] (spectral spillover effects limit its use for broad-band disturbances, see [3]). Nevertheless, as it will be shown in this paper, limited-band disturbances can be attenuated significantly by using an IIR internal model. To represent narrow-band disturbance peaks, a notch filter representation can be considered (see [4]). Notch filters have been extensively used in the estimation and/or rejection of narrow-band disturbances (for example, ANC in a diesel engine submarine in [5] or AVC for active magnetic bearings in [6]). One advantage of notch filters is that they can be tuned to represent various frequency width narrow-band signals. As such, they play a key role in the transition from narrow- to limited- and then to broad-

---

* Corresponding author.
E-mail address: tudor-bogdan.airimitoaie@u-bordeaux.fr (T.-B. Airimitoaie).

Acronyms		$\mathcal{H}$	Symbol used to denote the hypotheses considered in this article
ANC	Active noise control	IIR	Infinite impulse response
ANVC	Active noise and vibration control	IIRYK	Youla-Kučera parameterized IIR adaptive
AVC	Active vibration control		feedforward compensator using an IIR
dB	decibel		Youla-Kučera filter
FIR	Finite impulse response	IMP	Internal model principle
FIRYK	Youla-Kučera parameterized IIR adaptive	PAA	Parameter adaptation algorithm
	feedforward compensator using an FIR	PRBS	Pseudo random binary sequence
	Youla-Kučera filter	PSD	Power spectral density
FUPLR	Filtered-U pseudo linear regression	SPR	Strictly positive real (transfer function)
FUSBA	Filtered-U stability based algorithm	T_s	Sampling time (in seconds)
f_s	Sampling frequency of the discretized system (in Hz)	var	variance

band disturbances. Furthermore, including the "right amount" of attenuation band is of importance in the context of feedback control in order to limit the spectral spillover effect on the output sensitivity function.

The idea of combining these two approaches is not new. It was motivated by the fact that one may get better results in a number of situations than using either adaptive feedforward or adaptive feedback compensation alone. The combination of the two approaches is often called "hybrid" even if the term "combined feedback and feedforward" compensation is in our opinion more appropriate. From a control methodology point of view it seems reasonable to attenuate disturbances by feedback up to the level allowed by robustness constraints and then add the feedforward compensation. As first indicated in [7] for the case of fixed feedback control combined with adaptive feedforward, there is a strong interaction between the two loops which has to be taken into account. In fact, this interaction is even stronger when both the feedback and feedforward compensators are adaptive as it will be shown in this paper.

A combined control structure with two secondary sources is presented in [8] for an ANC system. The solution is shown to be able to solve the problem of non-minimum phase secondary path. Hybrid controller design is done using $\mathcal{H}_2/\mathcal{H}_\infty$ theory. But the system is not adaptive and its performance is questionable when significant changes in the characteristics of the disturbance occur.

In [9], a combined controller is evaluated in simulation on an ANC system. The adaptation is done using the FxLMS algorithm and the authors have proposed an original method of adapting the step size. Nevertheless, the simulated ANC system does not take into account the positive feedback coupling generally present in feedforward compensation (see [10] for a presentation of the positive feedback coupling). Furthermore, the filtering uses only the secondary path model without considering the influence of the feedback controller.

In [11], FuLMS algorithms with variable step size are used for both feedforward and feedback in order to reduce vibrations on a thin-walled structure. A reference filter is used to reduce the influence of the positive feedback.

In [12], it is shown that reconstruction of the reference signal for the feedback controller in what the authors call the "traditional combination method based hybrid system (tHybrid)" introduces a coupling between the adaptive feedforward and the adaptive feedback controllers which complicates the design. A "simplified" combination without reconstruction is proposed to alleviate this problem. Nevertheless, the inherent positive feedback coupling is not taken into account, which can also introduce a coupling between the feedforward and the feedback controllers.

A combined adaptive feedforward + fixed feedback controller taking into account the positive feedback coupling has been proposed in [7]. The novelty of the design is that the influence of the fixed feedback controller on the adaptive feedforward algorithm is analysed and algorithms assuring the stability of the proposed scheme are presented.

The Youla-Kučera parametrisation has been extensively studied in the control literature. In [13], a complete review of its applications in identification and controller design for adaptive and nonlinear systems is given. In [2], the authors show the suitability of this parametrisation for adaptive AVC systems design due to reduced complexity and simplified stability analysis. The Youla-Kučera parametrisation has two main components: a central stabilizing controller and an adaptive filter. One important characteristic for adaptive control is the type of filter that is used. FIRYK has the property that the closed-loop poles are assigned by the central controller. As such, the stability analysis is much more easy to do, however, this does not guarantee the absence of spillover effects and, to prevent this, a careful design of the central controller has to be done.

When using the IIRYK parametrization, part of the system poles are assigned by the central controller and the rest are introduced by the denominator of the IIRYK filter. These poles will be asymptotically inside the unit circle if a strict positive real (SPR) condition is satisfied. These additional poles allow to reduce the spillover effect and simplify the design of the central controller. Concerning adaptive feedforward compensation, it has been shown in [2, Section 13.4] that the use of IIRYK allows to reduce the number of parameters of the adaptive filter with respect to the FIRYK.

In this paper, a combined adaptive feedforward + adaptive feedback AVC system is proposed and evaluated on an experimental test-bench with strong mechanical coupling. Both feedforward and feedback controllers' design is done based on the IIR
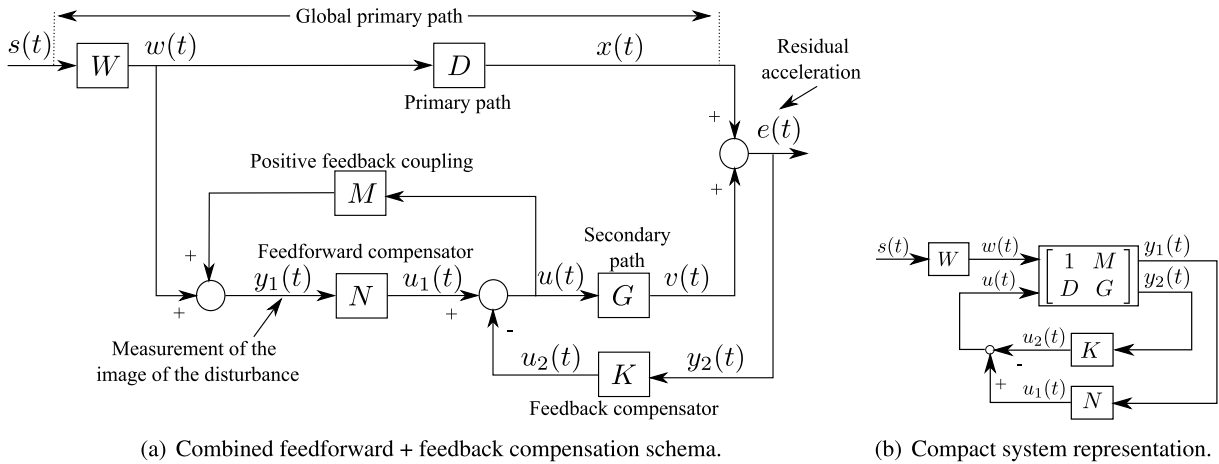
(a) Combined feedforward + feedback compensation schema.   (b) Compact system representation.

Fig. 1. Feedforward AVC with combined feedforward + feedback compensation.

Youla–Kučera (IIRYK) parametrization. A complete theory for the design of combined adaptive feedforward - adaptive feedback controllers is given. For practitioners of AVC, it also helps to understand the potential of feedback, feedforward, and combined feedforward-feedback approaches. By the various comparisons done, the paper also clarifies the pertinence of the use of combined feedforward - feedback approaches.

There are two intermediate theoretical contributions that lead to the proposed combined adaptive feedforward + adaptive feedback control algorithm. Firstly, a new direct adaptive feedback algorithm using the IIRYK parametrization is introduced. The interesting aspect of this algorithm is that it can be used for attenuation of limited-band disturbances without introducing unwanted amplifications in other frequency regions. This is an extension of the algorithm proposed in [2, Section 13.3] where only the numerator is adapted directly while for the denominator an indirect adaptation scheme is used. Secondly, an adaptive IIRYK feedforward compensator in the presence of a fixed feedback is also presented (this is an extension of the results given in [7]). The main contribution of the paper is the development of an adaptive feedforward + adaptive feedback compensation algorithm using IIRYK parametrization for which a specific stability analysis is provided.

The paper is organized as follows. In Section 2, the basic equations of the AVC system and notations used in this paper are introduced. In Section 3, the adaptive feedback control algorithm based on IIRYK is presented. The IIRYK parametrization of the feedforward controller in the presence of a fixed feedback is presented and analysed in Section 4. A modification of the feedforward algorithm's filtering is proposed in Section 5 to guarantee the stability of the combined adaptive feedforward + adaptive feedback compensation. Results obtained on a test-bench for active vibration control are discussed in Section 6. Section 7 concludes this paper.

2. Basic equations and notations

The detailed block diagram associated with an AVC system using combined feedback + feedforward control as well as the generalized feedback representation are given Fig. 1. In Fig. 1(a), $D = \frac{B_D}{A_D}, G = \frac{B_G}{A_G}, M = \frac{B_M}{A_M}$ represent the transfer operators associated with the primary, secondary and reverse paths (all asymptotically stable). $\widehat{B}_G, \widehat{A}_G, \widehat{B}_M$, and $\widehat{A}_M$ are the estimates of B_G, A_G, B_M, and A_M. W represents an unknown asymptotically stable disturbance filter, which is a part of the mechanical system. $s(t)$ is the external disturbance source, $w(t)$ is the correlated disturbance measurement (in the absence of the compensation), $x(t)$ is the output of the primary path (residual acceleration in the absence of compensation), $y_1(t)$ is the measured primary signal which is the sum between $w(t)$ and the effect of the control signal $u(t)$ filtered by the reverse path M, and $v(t)$ is the output of the secondary path (non measurable).

$\mathcal{H}_1$ In the rest of this paper, it is assumed that very good model estimates can be obtained by system identification techniques,[1] such that $\widehat{B}_G = B_G, \widehat{A}_G = A_G, \widehat{B}_M = B_M$, and $\widehat{A}_M = A_M$.

The following notation for polynomials is used throughout this paper: $P(q^{-1}) = p_0 + \sum_{i=1}^{n_P} p_i q^{-i} = p_0 + q^{-1}P^*(q^{-1})$. For the primary, secondary, and reverse paths, $b_0^D = b_0^G = b_0^M = 0$ and $a_0^D = a_0^G = a_0^M = 1$.

Let's consider a feedforward controller given by

$$N(q^{-1}) = \frac{R^f(q^{-1})}{S^f(q^{-1})} \tag{1}$$

---

[1] Earlier works (see [2]) have shown that very good model estimates can be obtained by system identification techniques using experimental data.

and a feedback controller given by

$$K(q^{-1}) = \frac{R^b(q^{-1})}{S^b(q^{-1})}. \tag{2}$$

The control signal applied to the secondary path is given by

$$u(t+1) = u_1(t+1) - u_2(t+1), \tag{3}$$

where $u_1(t)$ and $u_2(t)$ are, respectively, the output of the feedforward and the feedback controllers

$$u_1(t) = N(q^{-1}) y_1(t) \tag{4}$$

$$u_2(t) = K(q^{-1}) y_2(t) = K(q^{-1}) e(t). \tag{5}$$

In the previous equation, $e(t) = y_2(t)$ is the residual acceleration measurement, which needs to be minimized.

In this paper, a difference is made between narrow-band and limited- or broad-band disturbances. Narrow-band disturbances can be generally represented by a Dirac impulse $\delta(t)$ passed through a notch filter of the form (see also [2, Section 13.4])

$$\Upsilon_n(q^{-1}) = \prod_{i=1}^{n} \frac{D_i(\rho_{n_i}q^{-1})}{D_i(q^{-1})}, \ 0 < \rho_{n_i} < 1, \tag{6}$$

where $D_i(q^{-1}) = 1 + a_i q^{-1} + q^{-2}$ and $a_i = -2\cos\left(\frac{2\pi f_i}{f_s}\right)$. The roots of $D_i(q^{-1})$ lie on the unit circle (see also [4]). n is the number of narrow-band peaks and f_i are their frequencies (in Hz). ρ_{n_i} allows to obtain different amplitudes and bandwidths for the peaks. The roots of $D_i(\rho_{n_i}q^{-1})$ are strictly inside the unit circle but on the same radial lines as those of $D_i(q^{-1})$.

Limited- or broad-band disturbances can be represented as

$$x_b(t) = \Upsilon_b(q^{-1})\delta(t) = \frac{B_b(q^{-1})}{A_b(q^{-1})}\delta(t), \tag{7}$$

where the denominator $A_b(q^{-1})$ has well damped zeros.

The disturbances considered in this paper can be represented as[2]

$$x(t) = x_n(t) + x_b(t) = \left(\Upsilon_n + \Upsilon_b\right)\delta(t) = \frac{B_x}{A_x}\delta(t). \tag{8}$$

This disturbance model allows to define an extension of the well-known internal model principle for feedback control ([14]). A feedback controller can strongly attenuate a disturbance if it contains the model of the transfer function generating the disturbance.[3] This idea is used in the next section to design the adaptive feedback control algorithm. Experimental results are shown in Section 6.

3. Youla–Kučera parametrization of the feedback controller

In this section, the adaptive IIR Youla–Kučera parametrization of the feedback controller will be presented in the absence of the feedforward compensation.[4] The following IIRYK parametrization of the feedback controller is proposed

$$\widehat{K}(q^{-1}) = \frac{\widehat{R}^b(q^{-1})}{\widehat{S}^b(q^{-1})} = \frac{R_0^b \widehat{A}^b + A_G H_R^b H_S^b \widehat{B}^b}{S_0^b \widehat{A}^b - B_G H_R^b H_S^b \widehat{B}^b}, \tag{9}$$

where the IIR filter $\widehat{Q}^b(q^{-1}) = \frac{\widehat{B}^b(q^{-1})}{\widehat{A}^b(q^{-1})}$ is given by

$$\widehat{B}^b(q^{-1}) = \widehat{b}_0^b + \widehat{b}_1^b q^{-1} + \cdots + \widehat{b}_{n_{B^b}}^b q^{-n_{B^b}}, \tag{10}$$

$$\widehat{A}^b(q^{-1}) = 1 + \widehat{a}_1^b q^{-1} + \cdots + \widehat{a}_{n_{A^b}}^b q^{-n_{A^b}}. \tag{11}$$

$R_0^b(q^{-1})$, $S_0^b(q^{-1})$ are the polynomials of a central feedback stabilizing controller and $H_R^b(q^{-1})$, $H_S^b(q^{-1})$ are its fixed parts. $\widehat{Q}^b$ represents the IIRYK filter that needs to be computed.

The output sensitivity function is given by

$$\widehat{\Xi}_{yp}^b(q^{-1}) = \frac{A_G(q^{-1})\widehat{S}^b(q^{-1})}{\widehat{P}^b(q^{-1})} \tag{12}$$

---

[2] In some of the following equations, the parenthesis (q^{-1}) will be dropped to save space. For time-varying transfer operators, (t, q^{-1}) will become (t).

[3] In fact an asymptotic cancellation of the disturbance is obtained.

[4] For an introductory presentation of the Youla–Kučera parametrization, see [2].

Fig. 2. Feedback AVC with adaptive IIRYK parametrized controller.

where $\widehat{P}^b(q^{-1})$ defines the characteristic polynomial of the feedback loop

$$\widehat{P}^b = A_G \widehat{S}^b + B_G \widehat{R}^b = \widehat{A}^b (A_G S_0^b + B_G R_0^b) = \widehat{A}^b P^{b_0} \tag{13}$$

and P^{b_0} denotes the characteristic polynomial of the feedback loop with the central controller.

3.1. Development of the IIRYK adaptive feedback algorithm

The idea of using an IIRYK parametrization instead of an FIRYK parametrization came from the observation made in [2, Eq. (13.24), page 261] (see also Appendix A) that considering a poles-zeros representation of the disturbance through the use of notch filters as described in Section 2 allows: (i) to extend the band of disturbances which can be compensated around a central frequency and (ii) to provide an optimal attenuation using IMP combined with the assignment of additional closed-loop poles to the values of the zeros of the disturbance model. As indicated in the introduction, an attempt to use this approach has been considered in [2, Section 13.3] leading to a mixed direct/indirect adaptive algorithm. In this section, a direct adaptive algorithm is proposed for adjusting simultaneously the numerator and denominator of the IIRYK filter.

The development of the adaptive algorithm for the feedback controller will be done in the absence of the feedforward compensator. The equivalent block representation is shown in Fig. 2. The notation $\widehat{u}_2(t)$ is used to indicate that an adaptive controller is used to compute this control signal.

The following hypotheses are considered:

$\mathcal{H}_2$ The disturbance $x(t)$ contains only narrow- and limited-band signals and there exists a filter $Q^b(q^{-1}) = \frac{B^b(q^{-1})}{A^b(q^{-1})}$ of finite dimension that cancels asymptotically the effect of the disturbance $x(t)$ (see also Appendix A) and the characteristic polynomial of the feedback loop

$$P^b = A_G S^b + B_G R^b = A^b (A_G S_0^b + B_G R_0^b) = A^b P^{b_0} \tag{14}$$

is a Hurwitz polynomial.

$\mathcal{H}_3$ he effect of the measurement noise upon the measured residual error is neglected (deterministic context).

Let's begin by considering known constant disturbances. Under hypothesis $\mathcal{H}_2$, the constant parameters $\widehat{Q}^b(q^{-1}) = \frac{\widehat{B}^b(q^{-1})}{\widehat{A}^b(q^{-1})}$ filter is sufficient to attenuate the disturbances. Adaptive IIRYK filtering is then introduced to deal with unknown and time-varying disturbances $\widehat{Q}^b(t, q^{-1}) = \frac{\widehat{B}^b(t, q^{-1})}{\widehat{A}^b(t, q^{-1})} \left(= \frac{\widehat{B}^b(t)}{\widehat{A}^b(t)}\right)$.

Under hypothesis $\mathcal{H}_3$, the measured output of the system is given by

$$y_2(t) = \widehat{v}^\circ(t) + x(t), \tag{15}$$

where $\widehat{v}^\circ(t)$ denotes the secondary path output in the presence of an adaptive controller.[5]

The objective is to attenuate the frequency peaks in the disturbance signal $x(t)$ (represented by $x_n(t)$) with a minimum influence on the broad-band characteristics. The band-stop filter (BSF) approach proposed in [2, Section 13.4] is well suited for this

---

[5] In adaptive control, the superscript ° is used to denote signals computed with previous values of the adapted parameters. Here, it reflects the fact that the secondary path has an intrinsic delay of one sampling period.

as it was shown that the BSFs have a limited influence on the output and input sensitivity functions outside of the frequency region of attenuation.

In the absence of the feedforward compensator, $u_1(t) = 0$, the measured output of the system can also be characterized as the disturbance passed through the output sensitivity function obtained using the adaptive filter. Therefore the output of the system is given by

$$y_2(t+1) = \frac{A_G(q^{-1})\widehat{S}^b(q^{-1})}{\widehat{P}^b(q^{-1})} \cdot \frac{B_x(q^{-1})}{A_x(q^{-1})}\delta(t+1) = \frac{A_G\left(S_0^b\widehat{A}^b - B_GH_R^bH_S^b\widehat{B}^b\right)}{P^{b_0}\widehat{A}^b} \cdot \frac{B_x}{A_x}\delta(t+1) \tag{16}$$

$$= \frac{S_0^b\widehat{A}^b - B_GH_R^bH_S^b\widehat{B}^b}{P^{b_0}\widehat{A}^b} \cdot w_\delta(t+1) = \frac{S_0^b}{P^{b_0}} \cdot w_\delta(t+1) - \frac{B_G^*H_R^bH_S^b}{P^{b_0}}\frac{\widehat{B}^b}{\widehat{A}^b} \cdot w_\delta(t) \tag{17}$$

$$= w_1(t+1) - \frac{\widehat{B}^b}{\widehat{A}^b} \cdot w^f(t), \tag{18}$$

where

$$w_\delta(t+1) = A_G(q^{-1})\frac{B_x(q^{-1})}{A_x(q^{-1})} \cdot \delta(t+1) = A_Gy_2(t+1) - B_G\hat{u}_2(t+1)$$
$$= \hat{A}_Gy_2(t+1) - \hat{B}_G^*\hat{u}_2(t), \qquad \text{(using hypothesis } \mathcal{H}_1) \tag{19}$$

$$w_1(t+1) = \frac{S_0^b(q^{-1})}{P^{b_0}(q^{-1})} \cdot w_\delta(t+1), \tag{20}$$

$$w^f(t) = \frac{B_G^*(q^{-1})H_R^b(q^{-1})H_S^b(q^{-1})}{P^{b_0}(q^{-1})} \cdot w_\delta(t). \tag{21}$$

Let's consider the IIR band-stop filter $\frac{S_{BSF}}{P_{BSF}}$ that needs to be introduced in the output sensitivity function to provide the desired disturbance attenuation. It was shown in [2, Section 13.4] that the optimal denominator of the Youla–Kučera filter is given by $P_{BSF} = A^b$ and that the optimal B^b can be calculated by solving the following Bezout equation (see [2, Eq. (13.84)])

$$S_0^bA^b = H_S^bS_{BSF}S' + B_GH_R^bH_S^bB^b \implies S_0^b = \frac{H_S^bS_{BSF}S'}{A^b} + B_GH_R^bH_S^b\frac{B^b}{A^b}. \tag{22}$$

Replacing $S_0^b(q^{-1})$ from the previous equation in (17)

$$y_2(t+1) = \frac{1}{P^{b_0}}\left(\frac{H_S^bS_{BSF}S'}{A^b} + B_GH_R^bH_S^b\frac{B^b}{A^b}\right) \cdot w_\delta(t+1) - \frac{B_G^*H_R^bH_S^b}{P^{b_0}}\frac{\widehat{B}^b}{\widehat{A}^b} \cdot w_\delta(t) \tag{23}$$

$$= \zeta(t+1) + \frac{B_G^*H_R^bH_S^b}{P^{b_0}}\left(\frac{B^b}{A^b} - \frac{\widehat{B}^b}{\widehat{A}^b}\right) \cdot w_\delta(t). \tag{24}$$

In the last equation, $\zeta(t+1)$ tends asymptotically to zero (as it will be shown next). Attenuation is then obtained by letting the computed $\widehat{Q}^b = \frac{\widehat{B}^b}{\widehat{A}^b}$ be equal to the ideal Q^b.

Let's analyse $\zeta(t+1)$ to see that it goes to zero.

$$\zeta(t+1) = \frac{H_S^bS_{BSF}S'}{P^{b_0}A^b}A_G\left(\Upsilon_n + \Upsilon_b\right) \cdot \delta(t+1) \tag{25}$$

From [2, Section 13.4], the BSFs should be chosen as the inverse model of the narrow-band disturbances model

$$\frac{S_{BSF}}{P_{BSF}} = \frac{S_{BSF}}{A^b} = \Upsilon_n^{-1} = \prod_{i=1}^n \frac{D_i(q^{-1})}{D_i(\rho_{n_i}q^{-1})}. \tag{26}$$

One obtains

$$\zeta(t+1) = \frac{H_S^bS'}{P^{b_0}}\left[1 + \left(\prod_{i=1}^n \frac{D_i(q^{-1})}{D_i(\rho_{n_i}q^{-1})}\right)\Upsilon_b\right]A_G\delta(t+1) \tag{27}$$

The transfer function in (27) has all its poles strictly inside the unit circle because $\rho_{n_i} < 1$, $\forall i$, P^{b_0} is designed to have asymptotically stable roots and the limited- or broad-band disturbance model Υ_b is asymptotically stable. Therefore, the effect of $\delta(t+1)$ vanishes asymptotically which means that $\zeta(t+1)$ tends asymptotically to zero.

In the context of unknown and/or time-varying disturbances, adaptation is necessary. One can consider $\varepsilon^\circ(t + 1) = y_2(t + 1)$ (regulation problem, see Fig. 1) obtained with $\widehat{A}^b(t, q^{-1})$ and $\widehat{B}^b(t, q^{-1})$ as the *a priori* adaptation error[6]

$$\varepsilon^\circ(t+1) = \zeta(t+1) + \frac{B_G^* H_R^b H_S^b}{P^{b_0}} \left(\frac{B^b}{A^b} - \frac{\widehat{B}^b(t)}{\widehat{A}^b(t)} \right) \cdot w_\delta(t). \tag{28}$$

Lemma 1. *The a posteriori adaptation error is given by*

$$\varepsilon(t+1) = \frac{1}{A^b} \left[\mathbf{\Theta}_b^T - \widehat{\mathbf{\Theta}}_b^T(t+1) \right] \mathbf{\Phi}_b(t) + \zeta_f(t+1), \tag{29}$$

where

$$\mathbf{\Theta}_b^T = \left[b_0^b, \ \ldots, \ b_{n_{B^b}}^b, \ a_1^b, \ \ldots, \ a_{n_{A^b}}^b \right], \tag{30a}$$

$$\widehat{\mathbf{\Theta}}_b^T(t) = \left[\widehat{b}_0^b(t), \ \ldots, \ \widehat{b}_{n_{B^b}}^b(t), \ \widehat{a}_1^b(t), \ \ldots, \ \widehat{a}_{n_{A^b}}^b(t) \right], \tag{30b}$$

$$\mathbf{\Phi}_b^T(t) = \left[w^f(t), \ \ldots, \ w^f\left(t - n_{B^b} \right), \ -\widehat{u}_b^f(t-1), \ \ldots, \ -\widehat{u}_b^f\left(t - n_{A^b} \right) \right], \tag{30c}$$

$$\zeta_f(t) = \frac{1}{A^b} \zeta(t). \tag{30d}$$

b_i^b, a_i^b *are the coefficients of the optimal Q^b -filter and $\widehat{b}_i^b, \widehat{a}_i^b$ are the coefficients of the estimated $\widehat{Q}^b$ -filter.*
For a proof, see Appendix B.

Eq. (29) will be used to develop the adaptation algorithms neglecting the non-commutativity of the operators when $\widehat{\mathbf{\Theta}}_b$ is time-varying (however, an exact algorithm can be derived in such cases - see [15]). Filtering the vector $\mathbf{\Phi}_b^T(t)$ through an asymptotically stable filter $L(q^{-1}) = \frac{B_L}{A_L}$, (29) becomes

$$\varepsilon(t+1) = \frac{1}{A^b L} \left(\mathbf{\Theta}_b^T - \widehat{\mathbf{\Theta}}_b^T(t+1) \right) \mathbf{\Psi}_b(t) + \zeta_f(t+1), \tag{31}$$

$$\mathbf{\Psi}_b(t) = L(q^{-1})\mathbf{\Phi}_b(t). \tag{32}$$

Eq. (31) has the standard form of an *a posteriori* adaptation error which, using the results of [2], suggests to use for the estimation of the parameters of $\widehat{Q}^b(t, q^{-1})$ the following PAA:

$$\widehat{\mathbf{\Theta}}_b(t+1) = \widehat{\mathbf{\Theta}}_b(t) + \mathbf{F}_b(t)\mathbf{\Psi}_b(t)\varepsilon(t+1) \tag{33a}$$

$$\varepsilon(t+1) = \frac{\varepsilon^\circ(t+1)}{1 + \mathbf{\Psi}_b^T(t) \mathbf{F}_b(t) \mathbf{\Psi}_b(t)} \tag{33b}$$

$$\varepsilon^\circ(t+1) = w_1(t+1) - \widehat{\mathbf{\Theta}}_b^T(t) \mathbf{\Phi}_b(t) \tag{33c}$$

$$\mathbf{F}_b(t+1) = \frac{1}{\lambda_1^b(t)} \left[\mathbf{F}_b(t) - \frac{\mathbf{F}_b(t) \mathbf{\Psi}_b(t) \mathbf{\Psi}_b^T(t) \mathbf{F}_b(t)}{\frac{\lambda_1^b(t)}{\lambda_2^b(t)} + \mathbf{\Psi}_b^T(t) \mathbf{F}_b(t) \mathbf{\Psi}_b(t)} \right] \tag{33d}$$

$$1 \geq \lambda_1^b(t) > 0, \ 0 \leq \lambda_2^b(t) < 2, \ \mathbf{F}_b(0) > 0, \tag{33e}$$

where $\lambda_1^b(t)$ and $\lambda_2^b(t)$ give the possibility to obtain various profiles for the matrix adaptation gain $\mathbf{F}_b(t)$.

---

[6] In adaptive control and estimation, the predicted output at $t + 1$ can be computed either on the basis of the previous parameter estimates (*a priori*) or on the basis of the current parameter estimates (*a posteriori*).

3.2. Stability analysis

As shown in [2, Theorem 4.1], under the SPR argument for guaranteeing the stability of the adaptive algorithm, the filter $L(q^{-1})$ should be chosen such that

$$\frac{1}{A^b(z^{-1})L(q^{-1})} - \frac{\lambda_2^b}{2}, \ \max_t \left(\lambda_2^b(t)\right) \leq \lambda_2^b < 2 \tag{34}$$

be strictly positive real. The best solution is to choose $L = \frac{1}{A^b}$. With this choice for the filter L, asymptotic stability of the scheme will be assured provided that

$$H(z^{-1}) = \frac{\widehat{A}^b(z^{-1})}{A^b(z^{-1})} - \frac{\lambda_2^b}{2}, \ \max_t \left(\lambda_2^b(t)\right) \leq \lambda_2^b < 2 \tag{35}$$

is SPR. This condition will always be satisfied if the estimated $\widehat{A}^b(z^{-1})$ is close to $A^b(z^{-1})$. In Section 6, the estimated $\widehat{A}^b(t, q^{-1})$ at time t is used to adaptively filter the vector $\Phi_b(t)$.

3.3. Practical aspects

It is supposed that a central feedback stabilising controller is known (R_0^b, S_0^b and its fixed parts). The central controller is in general designed just to stabilize the feedback loop using for example pole placement (see [2, Chapter 7]). Parameters vector $\widehat{\Theta}_b(0)$ and regressor vector $\Psi_b(0)$ are initialized as null vectors of appropriate sizes.

An initial diagonal adaptation gain matrix $F_b(0) = igb \cdot I$ is chosen with positive igb value (usually smaller than 1).

The following procedure is applied at each sampling time for adaptive operation:

1. Get the measured output $y_2(t + 1)$ and the applied control $\widehat{u}_2(t)$ to compute $w_\delta(t + 1)$ using (19).
2. Compute $w_1(t + 1)$ and $w^f(t)$ using (20) and (21) with P^{b_0} given in (13).
3. Compute $\Phi_b(t)$ and $\Psi_b(t)$ using $w^f(t)$ and

$$\widehat{u}_b^f(t - 1) = \frac{B_G^*(q^{-1})H_R^b(q^{-1})H_S^b(q^{-1})}{P^{b_0}(q^{-1})} \cdot \widehat{u}_b(t - 1). \tag{36}$$

4. Estimate the parameters of the Q^b-filter using the PAA (33).
5. Compute $\widehat{u}_b(t + 1)$ using (see Fig. 2)

$$\widehat{A}^b(q^{-1})\widehat{u}_b(t + 1) = \widehat{B}^b(q^{-1})w_\delta(t + 1). \tag{37}$$

6. Compute and apply the control $\widehat{u}_2(t + 1)$ (see Fig. 2)

$$S_0^b(q^{-1})\widehat{u}_2(t + 1) = -R_0^b(q^{-1})y_2(t + 1) - H_S^b(q^{-1})H_R^b(q^{-1})\widehat{u}_b(t + 1). \tag{38}$$

For the filtering done at step 3 to obtain $\Psi_b(t)$, several options can be considered:

- Run the algorithm for a certain time using $L(q^{-1}) = 1$ to get an estimate of A^b and then use $L(q^{-1}) = \widehat{A}^b$.
- Update $L(q^{-1})$ at each sampling instant using the current estimate of $\widehat{A}^b(q^{-1})$.

4. Youla–Kučera parametrization of the feedforward controller

Let's consider the IIRYK parametrized feedforward controller described in [2, Chapter 16] that is introduced on top of a constant feedback controller $K(q^{-1}) = \frac{R_0^b}{S_0^b}$ already present in the control loop as in Fig. 3. From [2, Chapter 16], the feedforward compensator is parametrized as

$$\widehat{N}(q^{-1}) = \frac{\widehat{R}^f(q^{-1})}{\widehat{S}^f(q^{-1})} = \frac{R_0^f\widehat{A}^f - A_M H_R^f H_S^f \widehat{B}^f}{S_0^f\widehat{A}^f - B_M H_R^f H_S^f \widehat{B}^f}, \tag{39}$$
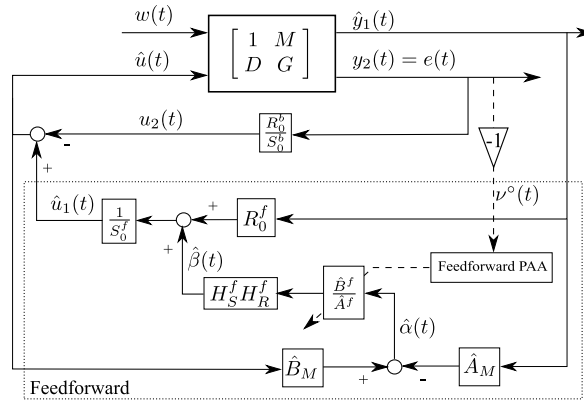
Fig. 3. Feedforward AVC with adaptive feedforward and fixed feedback compensators.

where the Youla–Kučera parameter is given by the IIR filter $\widehat{Q}^f(q^{-1}) = \frac{\widehat{B}^f(q^{-1})}{\widehat{A}^f(q^{-1})}$ with

$$\widehat{B}^f = \widehat{b}_0^f + \widehat{b}_1^f q^{-1} + \cdots + \widehat{b}_{n_{Bf}}^f q^{-n_{Bf}} \tag{40}$$

$$\widehat{A}^f = 1 + \widehat{a}_1^f q^{-1} + \cdots + \widehat{a}_{n_{Af}}^f q^{-n_{Af}}. \tag{41}$$

$R_0^f(q^{-1})$, $S_0^f(q^{-1})$ are the polynomials and $H_R^f(q^{-1})$, $H_S^f(q^{-1})$ are the fixed parts of a feedforward central (stabilizing) controller.

In the case of time-varying parameters, one has to consider the *a posteriori* output of the estimated feedforward compensator $\widehat{N}(t+1, q^{-1})$ using the IIRYK parametrization (see also [2, Chapter 16])

$$\widehat{u}_1(t+1) = \widehat{u}_1\left(t+1, \widehat{\boldsymbol{\Theta}}_f(t+1)\right) = -\left(\widehat{A}^f(t+1)S_0^f\right)^* \widehat{u}_1(t) + \widehat{A}^f(t+1)R_0^f \widehat{y}_1(t+1)$$
$$+ \widehat{B}^f(t+1)H_R^f H_S^f \cdot \left(B_M^* \widehat{u}_1(t) - A_M \widehat{y}_1(t+1)\right) \tag{42}$$

and the *a priori* output

$$\widehat{u}_1^\circ(t+1) = \widehat{u}_1(t+1, \widehat{\boldsymbol{\Theta}}_f(t))$$
$$= -\left(\widehat{A}^f(t)S_0^f\right)^* \widehat{u}_1(t) + \widehat{A}^f(t)R_0^f \widehat{y}_1(t+1) + \widehat{B}^f(t)H_R^f H_S^f \left(B_M^* \widehat{u}_1(t) - A_M \widehat{y}_1(t+1)\right), \tag{43}$$

where

$$\widehat{\boldsymbol{\Theta}}_f^T = \left[\widehat{b}_0^f, \ \ldots \ , \ \widehat{b}_{n_{Bf}}^f, \ \widehat{a}_1^f, \ \ldots \ , \ \widehat{a}_{n_{Af}}^f\right] \tag{44}$$

is the vector of parameters of the estimated $\widehat{Q}^f$ filter and $\widehat{y}_1(t)$ denotes the measurement of the image of the disturbance with positive coupling from a control signal computed using an adaptive controller.[7]

4.1. Development of the algorithms

The algorithms for adaptive feedforward compensation in the presence of a feedback controller will be developed under the hypotheses:

$\mathcal{H}_4$ The disturbance signal $w(t)$ is bounded (which is equivalent to say that $s(t)$ is bounded and $W(q^{-1})$ in Fig. 1 is asymptotically stable).

$\mathcal{H}_5$ There exist a central feedforward compensator $N_0(q^{-1})$ (R_0^f, S_0^f), which stabilizes the inner positive feedback loop formed by N_0 and M, and a central feedback compensator $K_0(q^{-1})$ (R_0^b, S_0^b) that stabilizes the closed-loop $(G - K)$ and the characteristic polynomials (i) of the inner positive loop

---

[7] In the feedforward + feedback scheme, the notation $\widehat{y}_1(t)$ implies that at least one of the two controllers is adaptive.

$$P^{f_0}(q^{-1}) = A_M(q^{-1})S_0^f(q^{-1}) - B_M(q^{-1})R_0^f(q^{-1}) \tag{45}$$

(ii) of the closed-loop $(G - K)$ $P^{b_0}(q^{-1})$ and (iii) of the coupled feedforward-feedback loop

$$P^{f_0 b_0} = A_M S_0^f \left(A_G S_0^b + B_G R_0^b \right) - B_M R_0^f S_0^b A_G \tag{46}$$

are Hurwitz.

$\mathcal{H}_6$ (Perfect matching condition) There exists a value of the Q^f parameters such that

$$\frac{G \cdot A_M (R_0^f A^f - A_M H_R^f H_S^f B^f)}{A^f (A_M S_0^f - B_M R_0^f)} = -D. \tag{47}$$

$\mathcal{H}_7$ The effect of the measurement noise upon the measurement of the residual acceleration is neglected (deterministic context).

A first step in the development of the algorithms is to establish a relation between the errors on the estimation of the parameters of the feedforward filter and the measured residual acceleration. This is summarized in the following lemma, where $\nu(t)$ denotes the *a posteriori* adaptation error. $\nu(t)$ can be computed from the *a priori* adaptation error which is given by $\nu^\circ(t) = -e(t)$ (see Fig. 3).

Lemma 2. *Under hypotheses $\mathcal{H}_4$, $\mathcal{H}_5$, $\mathcal{H}_6$, and $\mathcal{H}_7$, for the system described in* Section 2*, using an estimated IIR Youla–Kučera parameterized feedforward compensator with constant parameters and a fixed feedback controller K_0, one has:*

$$\nu(t+1) = \frac{A_M A_G S_0^b}{P^{f b_0}} G \left[\Theta_f - \widehat{\Theta}_f \right]^T \Phi_f(t) \tag{48}$$

where

$$\Theta_f^T = \left[b_0^f, \ \dots, \ b_{n_{B^f}}^f, \ a_1^f, \ \dots, \ a_{n_{A^f}}^f \right], \tag{49}$$

is the vector of parameters of the optimal Q^f-filter assuring perfect matching and $\Phi_f(t)$ is given by

$$\Phi_f^T(t) = [\alpha(t+1), \alpha(t), \dots, \alpha(t-n_{B_Q}+1), -\beta(t), -\beta(t-1), \dots, -\beta(t-n_{A_Q})], \tag{50}$$

with

$$\alpha(t+1) = B_M \widehat{u}_1(t+1) - A_M \widehat{y}_1(t+1) = B_M^* \widehat{u}_1(t) - A_M \widehat{y}_1(t+1) \tag{51a}$$

$$\beta(t) = S_0^f \widehat{u}_1(t) - R_0^f \widehat{y}_1(t). \tag{51b}$$

$P^{f b_0}$ in (48) is obtained from (46) by replacing the central feedforward controller $N_0(q^{-1})$ by the Youla–Kučera parametrized feedforward controller $N(q^{-1})$ given in (39).

The proof follows the same lines as in [2, Appendix D] and is not recalled here.

Corollary: *For $R^b = 0$ and $S^b = 1$ (absence of the feedback controller), the error equation for pure feedforward compensation given in [2, Chapter 16] is obtained*

$$\nu(t+1) = \frac{A_M}{P^f} G \left[\Theta_f - \widehat{\Theta}_f \right]^T \Phi_f(t) = \frac{A_M}{\widehat{A^f} P^{f_0}} G \left[\Theta_f - \widehat{\Theta}_f \right]^T \Phi_f(t), \tag{52}$$

where

$$P^f(q^{-1}) = A_M(q^{-1})S^f(q^{-1}) - B_M(q^{-1})R^f(q^{-1}) = \widehat{A^f}(q^{-1})P^{f_0}(q^{-1}). \tag{53}$$

Filtering the vector $\Phi(t)$ through an asymptotically stable filter $L(q^{-1}) = \frac{B_L}{A_L}$, (48) for $\widehat{\Theta} = $ constant becomes:

$$\nu(t+1) = \frac{A_M A_G S_0^b}{P^{f b_0} L} G [\Theta_f - \widehat{\Theta}_f]^T \Psi_f(t) \tag{54}$$

$$\Psi_f(t) = L(q^{-1}) \Phi_f(t). \tag{55}$$

Eq. (54) will be used to develop the adaptation algorithms neglecting the non-commutativity of the operators when $\widehat{\boldsymbol{\Theta}}_f$ is time-varying (however, an exact algorithm can be derived in such cases - see [15]).

Replacing the fixed estimated parameters by the current estimated parameters, (54) becomes the equation of the *a posteriori* residual (adaptation) error $v(t+1)$ (which is computed):

$$v(t+1, \widehat{\boldsymbol{\Theta}}(t+1)) = \frac{A_M A_G S_0^b}{P^{fb_0}L} G [\boldsymbol{\Theta}_f - \widehat{\boldsymbol{\Theta}}_f(t+1)]^T \boldsymbol{\Psi}_f(t). \tag{56}$$

(56) has the standard form for an *a posteriori* adaptation error ([2]), which immediately suggests to use the following PAA:

$$\widehat{\boldsymbol{\Theta}}_f(t+1) = \widehat{\boldsymbol{\Theta}}_f(t) + \mathbf{F}_f(t) \boldsymbol{\Psi}_f(t) v(t+1) \tag{57a}$$

$$v(t+1) = \frac{v^0(t+1)}{1 + \boldsymbol{\Psi}_f^T(t) \mathbf{F}_f(t) \boldsymbol{\Psi}_f(t)} \tag{57b}$$

$$\mathbf{F}_f(t+1) = \frac{1}{\lambda_1^f(t)} \left[\mathbf{F}_f(t) - \frac{\mathbf{F}_f(t) \boldsymbol{\Psi}_f(t) \boldsymbol{\Psi}_f^T(t) \mathbf{F}_f(t)}{\frac{\lambda_1^f(t)}{\lambda_2^f(t)} + \boldsymbol{\Psi}_f^T(t) \mathbf{F}_f(t) \boldsymbol{\Psi}_f(t)} \right] \tag{57c}$$

$$1 \geq \lambda_1^f(t) > 0, \ 0 \leq \lambda_2^f(t) < 2, \ \mathbf{F}_f(0) > 0, \tag{57d}$$

where $\lambda_1^f(t)$ and $\lambda_2^f(t)$ give the possibility to obtain various profiles for the matrix adaptation gain $\mathbf{F}_f(t)$ (see Section 6 and [2]).

4.2. Stability analysis

As shown in [2, Theorem 4.1], the stability of the system will depend on the characteristics of the transfer function $\frac{A_M A_G S_0^b}{P^{fb_0}L} G$ presented in (56). As stability requires that

$$H(z^{-1}) = \frac{A_M A_G S_0^b}{P^{fb_0}L} G - \frac{\lambda_2^f}{2}, \ \max_t \left(\lambda_2^f(t) \right) \leq \lambda_2^f < 2 \tag{58}$$

be *strictly positive real* (SPR), appropriate L filters should be chosen. Two choices for the filter *L* are considered, leading to the following algorithms:

Algorithm *FUPLR* (filtered-U pseudo linear regression):

$$L = \widehat{G}$$

In this case, (58) implies that

$$H(z^{-1}) = \frac{A_M A_G S_0^b}{P^{fb_0}} \frac{G}{\widehat{G}} - \frac{\lambda_2^f}{2} \tag{59}$$

has to be SPR.

Algorithm *FUSBA* (filtered-U stability based algorithm):

$$L = \frac{\widehat{A}_M \widehat{A}_G S_0^b}{\widehat{P}^{fb_0}} \widehat{G},$$

where

$$\widehat{P}^{fb_0} = A_M \widehat{S}^f (A_G S_0^b + B_G R_0^b) - B_M \widehat{R}^f S_0^b A_G \tag{60}$$

is an estimation of the characteristic polynomial of the coupled feedforward-feedback loop computed on the basis of available estimates of the parameters of the filter $\widehat{N}$. In this case, (58) implies that

$$H(z^{-1}) = \frac{\widehat{P}^{fb_0}}{P^{fb_0}} \frac{A_M A_G}{\widehat{A}_M \widehat{A}_G} \frac{G}{\widehat{G}} - \frac{\lambda_2^f}{2} = \frac{\widehat{P}^{fb_0}}{P^{fb_0}} \frac{A_M B_G}{\widehat{A}_M \widehat{B}_G} - \frac{\lambda_2^f}{2} \tag{61}$$

has to be SPR. Provided that the estimated polynomials are close enough to the real polynomials, using the *FUSBA*, the SPR condition will be satisfied (see [2, Chapter 16] for a similar analysis).

The algorithm analysis follows the same lines as in [2, Section 15.7 and Chapter 16] and will not be recalled here.

Remark 1. Replacing $\widehat{S}^f$ and $\widehat{R}^f$ from (39), (60) becomes

$$\widehat{P}^{fb_0} = \widehat{A}^f P^{f_0 b_0} - \widehat{B}^f A_M B_M H_R^f H_S^f B_G R_0^b. \tag{62}$$

As opposed to Section 3, the characteristic polynomial of the closed-loop can not be simply written based on only $\widehat{A}^f$ and $P^{f_0 b_0}$ (see (13)). It can be seen in (62) that the "positive coupling" (A_M, B_M) influences the poles of the feedback control loop. A modified version of the feedforward filter's parametrization is proposed in Appendix C in order that the characteristic polynomial of the closed-loop be not affected by the feedback.

Remark 2. In the absence of the positive feedback coupling ($B_M = 0$), (62) becomes $\widehat{P}^{fb_0} = \widehat{A}^f P^{f_0 b_0}$ which simplifies the design using the SPR stability condition.

4.3. Practical aspects

It is supposed that a central feedforward stabilising controller is known ($R_0^f(q^{-1})$, $S_0^f(q^{-1})$ and its fixed parts) and that the fixed feedback controller $K(q^{-1})$ is given. Parameters vector $\widehat{\boldsymbol{\Theta}}_f(0)$ and regressor vector $\boldsymbol{\Psi}_f(0)$ are initialized as null vectors of appropriate sizes.

An initial diagonal adaptation gain matrix $\mathbf{F}_f(0) = igf \cdot I$ is chosen with positive igf value (usually smaller than 1).

For the *FUSBA* algorithm, several options for updating $\widehat{P}^{fb_0}$ can be considered:

- Run Algorithm *FUPLR* for a certain time to get estimates of $\widehat{A}^b$, $\widehat{B}^b$, $\widehat{A}^f$, and $\widehat{B}^f$ and compute $\widehat{P}^{fb_0}$.
- Update $\widehat{P}^{fb_0}$ at each sampling instant or from time to time using Algorithm *FUSBA* (after a short initialization horizon using Algorithm *FUPLR*).

The following procedure is applied at each sampling time for adaptive operation:

1. Get the measured image of the disturbance $\widehat{y}_1(t + 1)$ and the applied control $\widehat{u}_1(t)$ to compute $\alpha(t + 1)$ and $\beta(t)$ using (51a) and (51b).
2. Compute $\boldsymbol{\Phi}_f(t)$ and $\boldsymbol{\Psi}_f(t)$ using (50) and (55).
3. Get the measured residual acceleration $e(t + 1)$ to compute $v^\circ(t + 1) = -e(t + 1)$ (see Fig. 3).
4. Estimate the parameters of the Q^f-filter using the PAA (57).
5. Compute using (42) and apply the control $\widehat{u}_1(t + 1)$ (see Fig. 3).

5. Adaptive feedforward + adaptive feedback Youla–Kučera control

In this section, in addition to the previous one, also the feedback controller's parameters are updated at each sampling instant. The combined adaptive feedforward + adaptive feedback control scheme is shown in Fig. 4. In the presence of the adaptive feedback controller $\widehat{K}$ from (9), (54) becomes

$$v(t + 1) = \frac{A_M A_G S^b}{P^{fb} L} G \left[\boldsymbol{\Theta}_f - \widehat{\boldsymbol{\Theta}}_f \right]^T \boldsymbol{\Psi}_f(t) = \frac{A_M B_G S^b}{P^{fb} L} \left[\boldsymbol{\Theta}_f - \widehat{\boldsymbol{\Theta}}_f \right]^T \boldsymbol{\Psi}_f(t). \tag{63}$$

The difference with the case of fixed feedback is that S_0^b and P^{fb_0} are replaced by S^b and P^{fb}. Taking into account (63), the stability conditions requires that

$$H(z^{-1}) = \frac{A_M A_G S^b}{P^{fb} L} G - \frac{\lambda_2^f}{2} = \frac{A_M B_G S^b}{P^{fb} L} - \frac{\lambda_2^f}{2}, \ \max_t \left(\lambda_2^f(t) \right) \le \lambda_2^f < 2 \tag{64}$$

be SPR. Two choices for the filter L are considered, leading to the following algorithms:
Algorithm *FUPLR* (filtered-U pseudo linear regression):

$$L = \widehat{G}$$

In this case, (64) implies that

$$H(z^{-1}) = \frac{A_M A_G S^b}{P^{fb}} \frac{G}{\widehat{G}} - \frac{\lambda_2^f}{2} \tag{65}$$
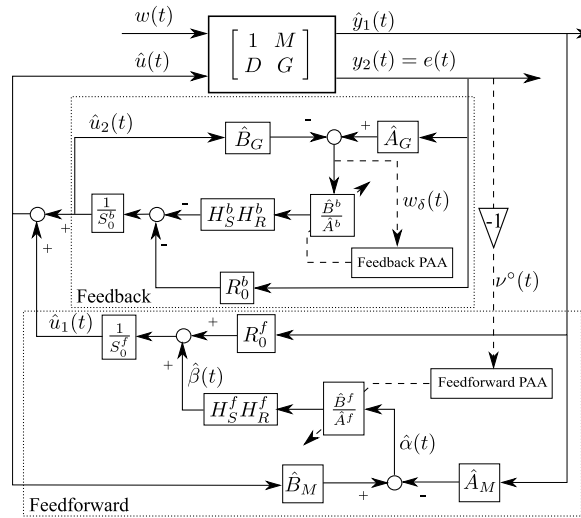
has to be SPR.

Fig. 4. Feedforward AVC with adaptive feedback and adaptive feedforward compensators.

Algorithm *FUSBA* (filtered-U stability based algorithm):

$$L = \frac{\widehat{A}_M \widehat{A}_G \widehat{S}^b}{\widehat{P}^{fb}} \widehat{G} = \frac{\widehat{A}_M \widehat{B}_G \widehat{S}^b}{\widehat{P}^{fb}}, \tag{66}$$

where

$$\widehat{P}^{fb} = \widehat{A}_M \widehat{S}^f (\widehat{A}_G \widehat{S}^b + \widehat{B}_G \widehat{R}^b) - \widehat{B}_M \widehat{R}^f \widehat{S}^b \widehat{A}_G. \tag{67}$$

The asymptotic stability of the system is assured if

$$H(z^{-1}) = \frac{A_M B_G S^b}{\widehat{A}_M \widehat{B}_G \widehat{S}^b} \cdot \frac{\widehat{P}^{fb}}{P^{fb}} - \frac{\lambda_2^f}{2}, \ \max_t \left(\lambda_2^f(t) \right) \le \lambda_2^f < 2 \tag{68}$$

is SPR. Provided that the estimated polynomials in (66) are close enough to the real polynomials, the SPR condition will be satisfied. Clearly the satisfaction of this condition will depend on the closeness of the real and estimated models (for $A_M, A_G,$ and B_G) and of the closeness of the P and $\widehat{P}$ polynomials.

Although FUPLR is straightforward to apply as only the model of the secondary path is used, it is more difficult to satisfy the SPR condition. It is recommended to use the FUSBA algorithm instead. Nevertheless, for the combined adaptive feedforward - adaptive feedback, both numerator and denominator of the feedback controller are needed for the SPR filtering.

To reduce the computational complexity, fixed feedback controller parameters are considered in the L filter for the FUSBA algorithm. These parameters can be obtained in two ways:

- Run algorithm FUPLR for a certain time and then use the estimates of the feedback controller parameters in the filter for FUSBA.
- Run the combined fixed feedforward + adaptive feedback algorithm for a certain time and then use the obtained feedback controller parameters in the FUSBA algorithm for the feedforward part.

The first approach has been used for the experimental evaluation presented in Section 6.

6. Experimental results

The AVC system used for experimental evaluation of the proposed algorithms is shown in Fig. 5 and a bloc diagram is given in Fig. 6(a). The system consists of 5 metallic plates (in dural of 1.8 Kg each one) connected by springs. The AVC system is suspended in the air with elastic cords (see Fig. 5(a)). The plates M1 and M3 are equipped with inertial actuators. The one on M1 serves as disturbance generator (inertial actuator I in Fig. 5(b)), the one on M3 serves for disturbance compensation (inertial actuator II in Fig. 5(b)). The system is equipped with a measure of the residual acceleration (on plate M3) and a measure of the image of the disturbance made by an accelerometer posed on plate M1. Due to the structure of this test-bench, an internal positive feedback coupling appears between the inertial actuator II and the disturbance image measured on M1. This coupling can have a destabilizing effect if not taken into account ([1,16]). Attempting to compensate it does not always provide good results because the compensation can not be perfect ([17,18]). Taking into account this positive coupling becomes even more important for

(a) Photo of the test-bench suspended by elastic cords.
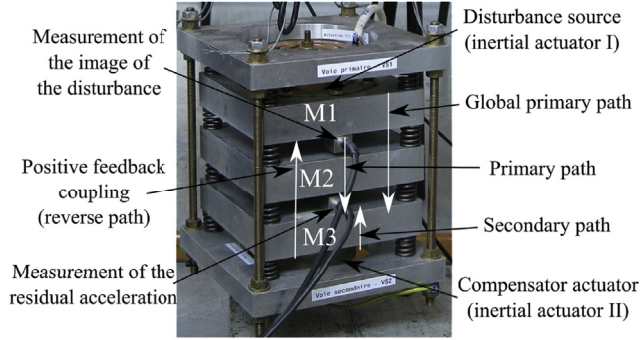
(b) Photo of the test-bench used for experimental evaluation.

Fig. 5. Active vibration control test-bench – photos.

(a) Bloc diagram of the experimental test-bench.
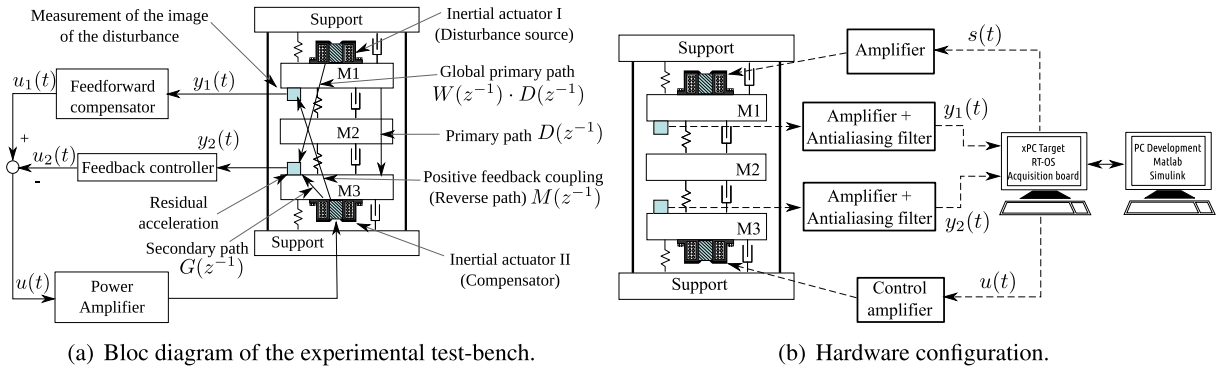
(b) Hardware configuration.

Fig. 6. Active vibration control test-bench – bloc diagram and hardware configuration.

combined feedforward + feedback control because of the effect of the feedback controller upon the measured image of the disturbance.

Fig. 6(a) shows a bloc diagram of the system with the feedforward and feedback controllers. The real-time implementation (see Fig. 6(b)) uses the MATLAB© xPC Target environment (R2009b). The PC for program development is a Dell© Optiplex 760. The PC target (Dell Optiplex GX270 with Pentium© 4 at 2.86 GHz) is equipped with input-output data acquisition board, analog-to-digital and digital-to-analog converters. A sampling frequency $f_s = 800$ Hz is used.

A detailed presentation of this test-bench and parametric identification results are given in [2]. The mechanical system in Fig. 5(b) has 6 resonant modes taking into account also the resonance of the elastic cords and those from the actuator. The identified model shows 6 vibration modes below 300 Hz with damping between 0.0042 and 0.655.[8] The identified frequency characteristics of the secondary and reverse path models can be analysed in Fig. 7. The mode at 258 with damping 0.655 is not visible on the diagram.[9]

Different experiments have been run to evaluate the proposed algorithms in the presence of broad-band disturbance. In all adaptive experiments, 20 parameters are used for the feedforward $\widehat{Q}^f$-filter ($n_{Af} = 10$ and $n_{Bf} = 9$) and 8 for the feedback $\widehat{Q}^b$-filter ($n_{Ab} = 4$ and $n_{Bb} = 3$). Decreasing gain adaptation algorithms are employed for both feedforward and feedback ($\lambda_1(t) = \lambda_2(t) = 1, \forall t \geq 0$) with initial gains $igb = 0.02$ and $igf = 0.01$. The excitation signal $s(t)$ sent from the xPC Target to the inertial actuator I is a PRBS with register length N = 10 and 0.15 amplitude.

Fig. 8 shows the power spectral density (PSD) of the disturbance in open-loop in the absence of the compensation (grey line). Also in Fig. 8, the PSD using the central feedforward controller (dotted line) is compared to the adaptive feedforward

---

[8] Experimental identification of the secondary path detected a supplementary 7th vibratory mode at 344 Hz. All the identified modes have been taken into account for the design of the central controller.
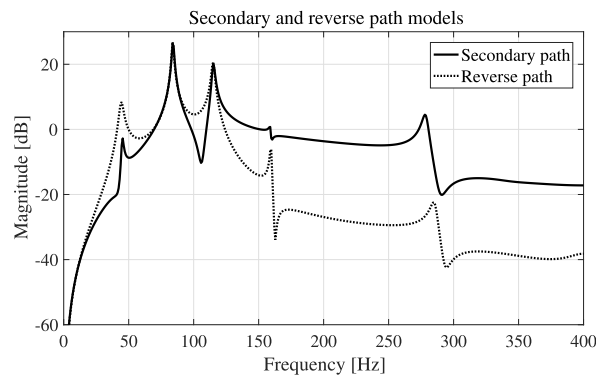
[9] Experimental data can be downloaded from: http://tudor-bogdan.airimitoaie.name/anvc.html.

Fig. 7. Frequency characteristics of the identified secondary and reverse path models.
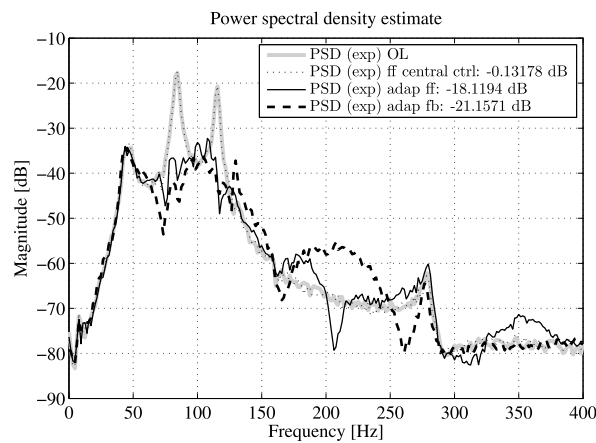

Fig. 8. Power spectral density comparison for the open-loop, central feedforward, adaptive feedback, and adaptive feedforward.

alone (solid black line) and the adaptive feedback controller alone (dashed line). The central feedforward controller is stabilizing the system but it does not introduce significant attenuation (PSD almost identical to the one of the disturbance). It is interesting to note that the attenuation of the adaptive feedback controller alone is better than that of the adaptive feedforward controller alone. An explanation for this is that in the proposed experimental test-bench the broad-band disturbance injected from the computer is passed through the mechanical system before reaching the residual acceleration measurement, acting as a filter that transforms the signal into a limited-band one with two major narrow-band peaks. Although limited by the Bode integral (waterbed) effect, the adaptive feedback controller introduces more attenuation on the two frequency peaks at 84 Hz and 116 Hz than the adaptive feedforward controller. Nevertheless, spillover effects can be observed around 200 Hz.

The global attenuation indicated in the PSD figures is computed using the variances of an open-loop and a closed-loop measured residual accelerations as $20\log_{10}\left(\frac{\text{var}(e(t))}{\text{var}(x(t))}\right)$. For each experiment, $x(t)$ is measured in open-loop and $e(t)$ is the residual acceleration in closed-loop with the corresponding controller. For the feedforward adaptive IIRYK, an attenuation of -18.12 dB is obtained, while for the feedback adaptive IIRYK controller the attenuation is of -21.16 dB. For the adaptive feedforward, the FUSBA algorithm of Subsection 4.2 is used with $S_0^b = 1$ and $R_0^b = 0$ (absence of the feedback controller).

In Fig. 9, the results with the combined feedback + feedforward control are provided. First, adaptive feedforward is evaluated in the presence of a fixed feedback controller. The fixed feedback is the equivalent feedback controller obtained using the parameters from the adaptive feedback test given in Fig. 8. An attenuation of -23.16 dB is obtained. In the second experiment, using both adaptive feedforward and adaptive feedback, -25.8 dB of attenuation are obtained. In both cases, the feedforward parametrization in (39) is implemented with the FUSBA algorithm using an approximated $\widehat{P}^{fb_0} = \widehat{A}^f P^f_0 b_0$ instead of the exact formula given in (62) (or (60)). In the case of the fixed feedback there is almost no difference between the phases of the two polynomials. For the adaptive feedforward + adaptive feedback, the maximum phase difference is of 28° (see Fig. 10) which is sufficient to guarantee the stability of the algorithm since the positive realness condition requires roughly that the phase difference between the exact $\widehat{P}^{fb_0}$ given by (62) and the approximated one in the filter of the regressor be less than 90°.
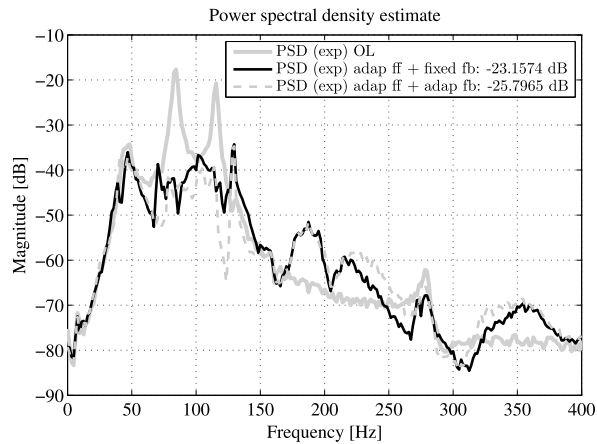
Fig. 9. Power spectral density comparison for the adaptive feedforward in the presence of fixed feedback or adaptive feedback.
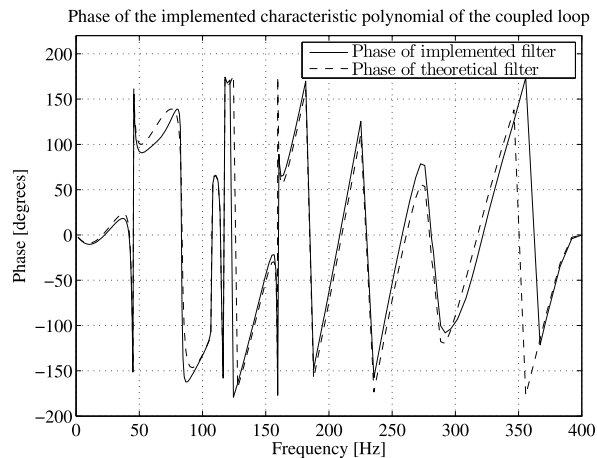

Fig. 10. Phase portrait comparison for theoretic and implemented characteristic polynomial for adaptive feedforward + adaptive feedback (FUSBA algorithm).

Table 1 gives a summary of the obtained results. Each experiment is started in open-loop for 50 s. This allows to compute the variance of the residual error in open-loop and later to compute the global attenuation for the corresponding experiment.

To demonstrate the adaptation capabilities of the proposed control scheme, the disturbance $s(t)$ sent from the computer changes its characteristics by the use of two different filters. The frequency responses of these filters are shown in Fig. 11(a). Before 212 s a low-pass filter with 100 Hz cut-off frequency is used. After 212 s, a high-pass filter with the same cut-off frequency is used instead. The frequency domain comparison of the two disturbances (in open-loop) is given in Fig. 11(b). Experimental results are shown in Fig. 12. In Fig. 12(a), the adaptation is stopped at 200 s and the algorithm is not capable of attenuating the disturbance. In Fig. 12(b), the adaptation is active and the controller is capable of reducing the disturbance even after the change at 212 s.

Table 1
Experimental comparison of the algorithms.

|	Open-loop var. $var(x(t))$	Closed-loop var. $var(\epsilon^\circ(t))$	Global att. (dB)
Feedforward central controller	0.05008	0.04933	−0.13178
Adaptive feedforward	0.04977	0.00618	−18.1194
Adaptive feedback	0.04943	0.00433	−21.1571
Adaptive feedforward + fixed feedback	0.04949	0.00344	−23.1574
Adaptive feedforward + adaptive feedback	0.04975	0.00255	−25.7965

(a) Filters frequency responses.   (b) PSD comparison of the disturbance sequences.
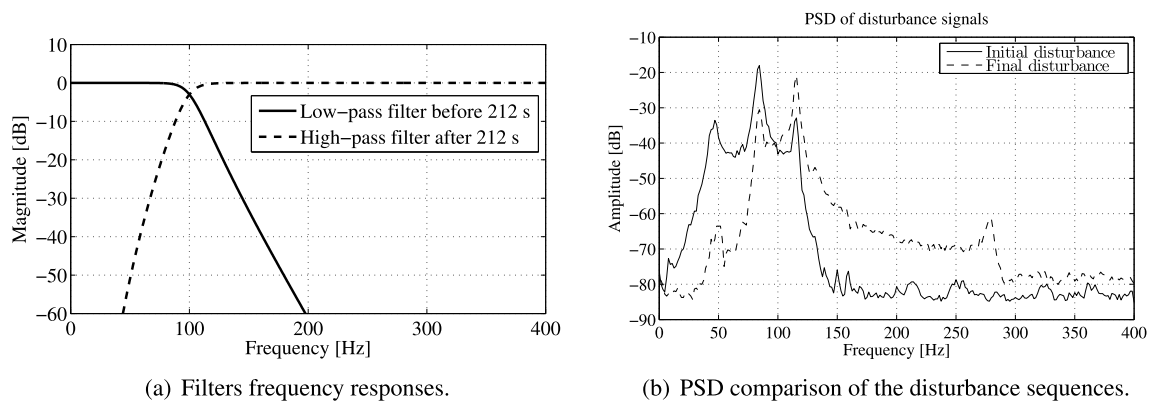
Fig. 11. Filter frequency responses (a) and PSD of the disturbance sequences (b).

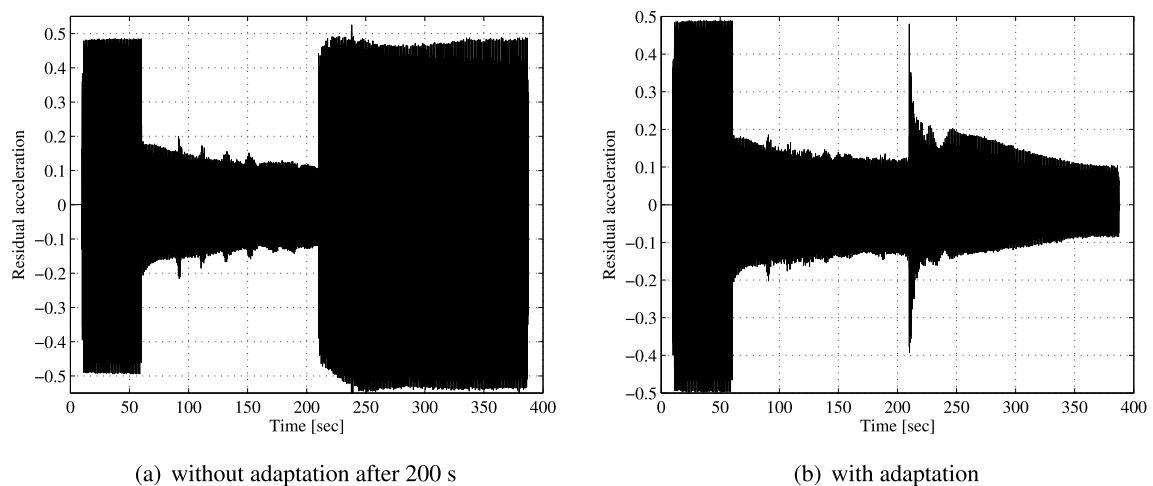(a) without adaptation after 200 s   (b) with adaptation

Fig. 12. Residual acceleration for algorithm FUSBA for a time-varying disturbance signal.

7. Conclusions

Three new algorithms for AVC based on the Youla-Kučera parametrizations of the feedback and the feedforward controllers are proposed and analysed in this paper.

A first contribution is the design of a feedback adaptive controller. This algorithm has the benefit that no secondary accelerometer is needed to measure an upstream image of the disturbance. The use of the Youla-Kučera parametrization allows to obtain very good attenuation results even with a small number of adapted parameters as can be seen in the experimental evaluation. The IIRYK adaptive feedback can offer better results and its implementation is much simpler than that of an adaptive feedforward for the case of limited-band signals.

For systems where an upstream measurement of the residual acceleration is available, two algorithms combining feedforward and feedback are also proposed. The paper presents first the adaptive feedforward in the presence of a fixed feedback. Finally, it is shown that in the presence of an adaptive feedback, the stability conditions for the feedforward part change. New stable algorithms are proposed and analysed. The paper has shown that the proposed algorithms for adaptive feedforward + adaptive feedback allow to outperform the adaptive feedforward and the adaptive feedforward + fixed feedback algorithms. In addition, these new algorithms are backed up by a complete stability analysis and take into account the strong coupling between feedback and feedforward for guaranteeing the stability.

It is worth mentioning that the presented methods have the potential of being used in various applications of AVC. A possible approach for a practitioner could be to try them in the order of presentation in this article, i.e. begin with the adaptive feedback and then try the combined schemes. Selection of the good configuration for the compensation of disturbances is problem dependent. While the combined adaptive feedback + adaptive feedforward provides the best results, for specific types of disturbances intermediate configurations may provide good enough performance.

Acknowledgements

Appendix A Internal model principle for the notch filter disturbance model

Let's suppose that the disturbance $x_n(t)$ is composed of a single narrow-band peak. From Section 2, $x_n(t)$ is given by

$$x_n(t) = \frac{D(\rho_n z^{-1})}{D(z^{-1})} \cdot \delta(t), \tag{A.1}$$

where $\alpha = -2\cos\left(2\pi\omega_d T_s\right)$ and ω_d is the frequency of the disturbance in Hz. $D(\rho_n z^{-1})$ is given by:

$$D(\rho_n z^{-1}) = 1 + \rho_n \alpha z^{-1} + \rho_n^2 z^{-2}, \tag{A.2}$$

with $0 < \rho_n < 1$. The roots of $D(\rho_n z^{-1})$ are on the same radial line as those of $D(z^{-1})$ but inside of the unit circle and therefore stable [4].

Fig. A.13 shows notch filter frequency responses obtained for different values of ρ_n. It is clear that the representation (A.1) is well suited for describing narrow-band disturbances with different frequency widths which is of interest in the context of the present paper.
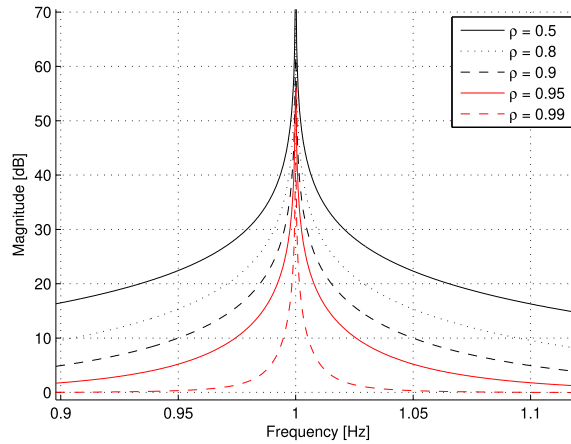

Fig. A.13. Magnitude plot frequency responses of a notch filter for various values of the parameter ρ.

Using (9) and (12), the output of the plant in the presence of the disturbance can be expressed as

$$y_2(t) = \frac{A_G \widehat{S}^b}{\widehat{P}^b} \cdot \frac{D(\rho_n q^{-1})}{D(q^{-1})} e(t) = \frac{A_G}{P_0^b} \cdot \frac{S_0^b \widehat{A}^b - B_G H_R^b H_S^b \widehat{B}^b}{\widehat{A}^b} \cdot \frac{D(\rho_n q^{-1})}{D(q^{-1})} \cdot e(t). \tag{A.3}$$

In order to minimize the effect of the disturbance, one should minimize the variance of $y_2(t)$. From the IMP, as it is shown in [2, Eqs. (13.81)–(13.85)], there exists a polynomial $\widehat{B}^b$ so that $D(q^{-1})$ can be included in $\widehat{S}^b = S_0^b \widehat{A}^b - B_G H_R^b H_S^b \widehat{B}^b$. This assures the asymptotic cancellation of the disturbance in a deterministic context. Choosing $\widehat{A}^b$ equal to $D(\rho_n q^{-1})$ assures the minimization of the effect of the disturbance (see [2, Section 3.4]).

Appendix B Proof of Lemma 1

Observing that

$$u_b(t) = \frac{B^b(q^{-1})}{A^b(q^{-1})} \cdot w_\delta(t) = B^b(q^{-1}) w_\delta(t) - A^{b*}(q^{-1}) u_b(t-1) \tag{B.1}$$

$$= B^b w_\delta(t) - A^{b*} \widehat{u}_b(t-1) - A^{b*} \left[u_b(t-1) - \widehat{u}_b(t-1)\right] \tag{B.2}$$

and also

$$\widehat{u}_b(t) = \widehat{B}^b(t, q^{-1}) \cdot w_\delta(t) - \widehat{A}^{b*}(t, q^{-1}) \widehat{u}_b(t-1), \tag{B.3}$$

(28) becomes

$$\varepsilon^\circ(t+1) = \zeta(t+1) + \frac{B_G^* H_R^b H_S^b}{P^{b_0}} \left[\left(B^b - \widehat{B}^b(t) \right) \cdot w_\delta(t) - \left(A^{b*} - \widehat{A}^{b*}(t) \right) \widehat{u}_b(t-1) \right] - \frac{B_G^* H_R^b H_S^b}{P^{b_0}} \left[A^{b*} \left(u_b(t-1) - \widehat{u}_b(t-1) \right) \right]. \tag{B.4}$$

One can also define the *a posteriori* error

$$\varepsilon(t+1) = \zeta(t+1) + \frac{B_G^* H_R^b H_S^b}{P^{b_0}} \left[\left(B^b - \widehat{B}^b(t+1) \right) \cdot w_\delta(t) - \left(A^{b*} - \widehat{A}^{b*}(t+1) \right) \widehat{u}_b(t-1) \right]$$
$$- \frac{B_G^* H_R^b H_S^b}{P^{b_0}} \left[A^{b*} \left(u_b(t-1) - \widehat{u}_b(t-1) \right) \right]. \tag{B.5}$$

It is necessary to find an expression relating the difference $(u_b(t-1) - \widehat{u}_b(t-1))$ to the *a posteriori* error. Under the assumption that the ideal Youla–Kučera compensator $\frac{B^b(q^{-1})}{A^b(q^{-1})}$ completely cancels out the disturbance $x(t)$ (hypothesis $\mathcal{H}_2$), (15) becomes

$$y_2(t) = \widehat{v}^\circ(t) - v(t), \tag{B.6}$$

where $v(t) = -x(t)$ is the process output with the ideal IIRYK compensator. Observing that

$$\widehat{v}^\circ(t) = -\frac{B_G}{A_G} \frac{1}{S_0^b} \left[R_0^b y_2(t) + H_R^b H_S^b \widehat{u}_b(t) \right] \tag{B.7}$$

and

$$v(t) = -\frac{B_G}{A_G} \frac{1}{S_0^b} \left[0 + H_R^b H_S^b u_b(t) \right] \tag{B.8}$$

and subtracting these last two equation, one obtains

$$y_2(t) = -\frac{B_G}{A_G} \frac{R_0^b}{S_0^b} \cdot y_2(t) + \frac{B_G^*}{A_G} \frac{H_R^b H_S^b}{S_0^b} \left(u_b(t-1) - \widehat{u}_b(t-1) \right) \tag{B.9}$$

$$\left[1 + \frac{B_G}{A_G} \frac{R_0^b}{S_0^b} \right] \cdot y_2(t) = \frac{B_G^* H_R^b H_S^b}{A_G S_0^b} \left(u_b(t-1) - \widehat{u}_b(t-1) \right), \tag{B.10}$$

$$y_2(t) = \frac{B_G^* H_R^b H_S^b}{P^{b_0}} \left(u_b(t-1) - \widehat{u}_b(t-1) \right) \tag{B.11}$$

We introduce also the notation

$$\widehat{u}_b^f(t-1) = \frac{B_G^*(q^{-1}) H_R^b(q^{-1}) H_S^b(q^{-1})}{P^{b_0}(q^{-1})} \cdot \widehat{u}_b(t-1). \tag{B.12}$$

Turning back to (B.5) and using (21), one obtains

$$\varepsilon(t+1) = \zeta(t+1) + \left[B^b - \widehat{B}^b(t+1) \right] w^f(t) - \left[A^{b*} - \widehat{A}^{b*}(t+1) \right] \widehat{u}_b^f(t-1) - A^{b*} \varepsilon(t), \tag{B.13}$$

where it has also been considered that $\varepsilon(t) = y_2(t)$ since $\widehat{B}^b(t, q^{-1})$ and $\widehat{A}^{b*}(t, q^{-1})$ are used.

Thus the equation for the *a posteriori* error becomes

$$\varepsilon(t+1) = \frac{1}{A^b} \left[\boldsymbol{\Theta}_b^T - \widehat{\boldsymbol{\Theta}}_b^T(t+1) \right] \boldsymbol{\Phi}_b(t) + \zeta_f(t+1), \tag{B.14}$$

where $\boldsymbol{\Theta}_b$, $\widehat{\boldsymbol{\Theta}}_b(t+1)$, $\boldsymbol{\Phi}_b(t)$, and $\zeta_f(t+1)$ are given in (30).

Appendix C. Exact feedforward Youla–Kučera parametrization

In this appendix, a modified parametrization of the feedforward controller is proposed. As it will be shown, the new equations have the advantage that the characteristic polynomial can be written as the product of the IIR Youla–Kučera filter's denominator and the characteristic polynomial computed only using the feedforward and feedback central controllers.

Let's consider the following form for the feedforward filter parametrization

$$\widehat{N}(q^{-1}) = \frac{\widehat{R}^f(q^{-1})}{\widehat{S}^f(q^{-1})}, \tag{C.1}$$

with

$$\widehat{R}^f = R_0^f \widehat{A^f} - A_M H_R^f H_S^f \left(S^b A_G + R^b B_G \right) \widehat{B^f},$$ (C.2)

$$\widehat{S^f} = S_0^f \widehat{A^f} - B_M H_R^f H_S^f S^b A_G \widehat{B^f}.$$ (C.3)

Introducing the previous equations into (60), after some calculations, one obtains

$$\widehat{P^{f b_0}} = \widehat{A^f} P^{f_0 b_0}.$$ (C.4)

References

[1] J. Zeng, R. de Callafon, Recursive filter estimation for feedforward noise cancellation with acoustic coupling, J. Sound Vib. 291 (3–5) (2006) 1061–1079.
[2] I.D. Landau, T.-B. Airimitoae, A. Castellanos Silva, A. Constantinescu, Adaptive and Robust Active Vibration Control—methodology and Tests, Advances in Industrial Control, Springer Verlag, 2017.
[3] A. Xie, D. Bernstein, On spatial spillover in feedforward and feedback noise control, J. Sound Vib. 391 (2017) 1–19.
[4] A. Nehorai, A minimal parameter adaptive notch filter with constrained poles and zeros, IEEE Trans. Acoust. Speech Signal Process. ASSP 33 (1985) 983–996.
[5] D. Sachau, S. Jukkert, N. Hövelmann, Development and experimental verification of a robust active noise control system for a diesel engine in submarines, J. Sound Vib. 375 (Supplement C) (2016) 1–18.
[6] Q. Chen, G. Liu, B. Han, Unbalance vibration suppression for AMBs system using adaptive notch filter, Mech. Syst. Signal Process. 93 (Supplement C) (2017) 136–150.
[7] M. Alma, I.D. Landau, T.-B. Airimitoae, Adaptive feedforward compensation algorithms for AVC systems in the presence of a feedback controller, Automatica 48 (10) (2012) 982–985.
[8] J. Yuan, A hybrid active noise controller for finite ducts, Appl. Acoust. 65 (1) (2004) 45–57.
[9] L. Mokhtarpour, H. Hassanpour, A self-tuning hybrid active noise control system, J. Franklin Inst. 349 (5) (2012) 1904–1914 special Section on Nonlinear Multiresolution algorithms and Applications.
[10] S. Kuo, D. Morgan, Active noise control: a tutorial review, Proc. IEEE 87 (6) (1999) 943–973.
[11] L. Xie, Z. cheng Qiu, X. min Zhang, Analysis and experiments of adaptive feedforward and combined vibration control system with variable step size and reference filter, Aero. Sci. Technol. 61 (2017) 109–120.
[12] L. Wu, X. Qiu, I.S. Burnett, Y. Guo, Decoupling feedforward and feedback structures in hybrid active noise control systems for uncorrelated narrowband disturbances, J. Sound Vib. 350 (2015) 1–10.
[13] B. Anderson, From Youla–Kučera to identification, adaptive and nonlinear control, Automatica 34 (12) (1998) 1485–1506.
[14] B. Francis, W. Wonham, The internal model principle of control theory, Automatica 12 (5) (1976) 457–465.
[15] I.D. Landau, R. Lozano, M. M'Saad, A. Karimi, Adaptive Control, second ed., Springer, London, 2011.
[16] S. Elliott, T. Sutton, Performance of feedforward and feedback systems for active control, Speech Audio Process. IEEE Trans. 4 (3) (1996) 214–223.
[17] A. Wang, W. Ren, Convergence analysis of the filtered-U algorithm for active noise control, Signal Process. 83 (2003) 1239–1254.
[18] M. Bai, H. Lin, Comparison of active noise control structures in the presence of acoustical feedback by using the H_∞ synthesis technique, J. Sound Vib. 206 (1997) 453–471.